

Mass Measurement of Upper fp -Shell $N = Z - 2$ and $N = Z - 1$ Nuclei and the Importance of Three-Nucleon Force along the $N = Z$ Line

M. Wang^{1,2}, Y. H. Zhang^{1,2,*}, X. Zhou^{1,2}, X. H. Zhou^{1,2,†}, H. S. Xu^{1,2}, M. L. Liu¹, J. G. Li¹, Y. F. Niu^{3,4}, W. J. Huang^{1,5}, Q. Yuan⁶, S. Zhang⁶, F. R. Xu^{6,‡}, Yu. A. Litvinov^{1,7}, K. Blaum⁸, Z. Meisel⁹, R. F. Casten¹⁰, R. B. Cakirli¹¹, R. J. Chen^{1,7}, H. Y. Deng^{1,2}, C. Y. Fu¹, W. W. Ge¹, H. F. Li^{1,2}, T. Liao^{1,2}, S. A. Litvinov^{7,1}, P. Shuai¹, J. Y. Shi^{1,2}, Y. N. Song^{1,2}, M. Z. Sun¹, Q. Wang^{1,2}, Y. M. Xing¹, X. Xu¹, X. L. Yan¹, J. C. Yang^{1,2}, Y. J. Yuan^{1,2}, Q. Zeng¹² and M. Zhang^{1,2}

¹CAS Key Laboratory of High Precision Nuclear Spectroscopy, Institute of Modern Physics, Chinese Academy of Sciences, Lanzhou 730000, China

²School of Nuclear Science and Technology, University of Chinese Academy of Sciences, Beijing 100049, China

³School of Nuclear Science and Technology, Lanzhou University, Lanzhou 730000, China

⁴Frontiers Science Center for Rare isotope, Lanzhou University, Lanzhou 730000, China

⁵Advanced Energy Science and Technology Guangdong Laboratory, Huizhou, 516007, China

⁶State Key Laboratory of Nuclear Physics and Technology, School of Physics, Peking University, Beijing 100871, People's Republic of China

⁷GSI Helmholtzzentrum für Schwerionenforschung, Planckstraße 1, 64291 Darmstadt, Germany

⁸Max-Planck-Institut für Kernphysik, Saupfercheckweg 1, 69117 Heidelberg, Germany

⁹Institute of Nuclear and Particle Physics, Department of Physics and Astronomy, Ohio University, Athens, Ohio 45701, USA

¹⁰Wright Nuclear Structure Laboratory, Yale University, New Haven, Connecticut 06520-8124, USA

¹¹Department of Physics, Istanbul University, Istanbul 34134, Turkey

¹²School of Nuclear Science and Engineering, East China University of Technology, Nanchang 330013, China



(Received 24 November 2022; revised 1 March 2023; accepted 17 March 2023; published 9 May 2023)

Using a novel method of isochronous mass spectrometry, the masses of ^{62}Ge , ^{64}As , ^{66}Se , and ^{70}Kr are measured for the first time, and the masses of ^{58}Zn , ^{61}Ga , ^{63}Ge , ^{65}As , ^{67}Se , ^{71}Kr , and ^{75}Sr are redetermined with improved accuracy. The new masses allow us to derive residual proton-neutron interactions (δV_{pn}) in the $N = Z$ nuclei, which are found to decrease (increase) with increasing mass A for even-even (odd-odd) nuclei beyond $Z = 28$. This bifurcation of δV_{pn} cannot be reproduced by the available mass models, nor is it consistent with expectations of a pseudo-SU(4) symmetry restoration in the fp shell. We performed *ab initio* calculations with a chiral three-nucleon force (3NF) included, which indicate the enhancement of the $T = 1$ pn pairing over the $T = 0$ pn pairing in this mass region, leading to the opposite evolving trends of δV_{pn} in even-even and odd-odd nuclei.

DOI: [10.1103/PhysRevLett.130.192501](https://doi.org/10.1103/PhysRevLett.130.192501)

Nuclear binding energy, $B(Z, N)$, derived directly from atomic masses, embodies the sum of all nucleonic interactions inside a nucleus with Z protons and N neutrons. Binding energy differences can isolate specific classes of interactions and provide hints on nuclear structure modifications [1,2]. Indeed, pairing correlations and shell closures were discovered through one- and two-nucleon separation energies. An important mass filter, the double binding energy difference denoted as δV_{pn} , has been used to isolate the residual proton-neutron (pn) interactions [3–5], and to sensitively probe a variety of structure phenomena, such as the onset of collectivity and deformation [6–9], changes of underlying shell structure [10], and phase transitional behavior [7,11]. Systematic surveys have revealed that δV_{pn} values can abruptly change when crossing shell closures [4,12,13]. Explained in terms of the

evolution of proton and neutron orbital overlaps, this was confirmed in the region near ^{208}Pb and ^{56}Ni [14,15].

It is well known [6] that the δV_{pn} values are considerably enhanced for $N = Z$ nuclei as compared to nearby nuclei with $N \neq Z$. Such enhancements in light sd -shell nuclei were interpreted in terms of the Wigner's SU(4) symmetry [5], which is broken in the heavier sd -shell nuclei due to increasing spin-orbit and Coulomb interactions. In the upper fp shell, a pseudo-SU(4) symmetry may be restored [16], leading to a restrengthening of δV_{pn} with increasing A . It is of basic importance for our understanding of the nuclear force to verify or disprove its restoration in heavy $N \approx Z$ nuclei. To date, a trend towards increased δV_{pn} beyond $Z = 29$ has been observed in odd-odd $N = Z$ nuclei [17,18], while data are still lacking for the even-even ones. In order to verify the theoretical expectations,

masses of heavy $N = Z - 2$ nuclei beyond $Z = 30$ are required [13,16,19].

For very proton-rich upper fp -shell nuclei, δV_{pn} can no longer be treated as small, since it has the same magnitude as the binding energies of the valence nucleons. In addition, a sufficient number of valence nucleons occupy identical orbits and may give pn correlations different from those observed nearer stability. In regions with extremely asymmetric N/Z ratios, three-nucleon forces (3NFs) are known to provide repulsive contributions to neutron-neutron (nn) and proton-proton (pp) interactions [20,21], which are essential for the emergence of new magic numbers [20], and in determining neutron and proton driplines [21]. The impact of 3NF on $B(Z, N)$ has been revealed for the neutron-deficient nuclei in sd and lower fp shells [22] and around ^{100}Sn [23].

In this Letter, we report accurate masses of $N = Z - 2$ and $N = Z - 1$ nuclei extending the δV_{pn} systematics to the upper fp shell. Surprisingly, we find opposite evolving trends of δV_{pn} in even-even and odd-odd nuclei.

The experiment was conducted at the Heavy Ion Research Facility in Lanzhou (HIRFL). A $^{78}\text{Kr}^{19+}$ beam accelerated to an energy of 460 MeV/u was fragmented on a 15 mm thick beryllium target at the entrance of the fragment separator RIBLL2 [24,25]. Reaction fragments emerging from the target were fully stripped. They were in-flight separated with RIBLL2 and injected into the experimental cooler storage ring (CSRe). The CSRe was tuned to the isochronous mode with the transition point $\gamma_t = 1.352$ [26–28]. The momentum acceptance of the CSRe is $\pm 0.33\%$. The RIBLL2-CSRe system was set to a fixed magnetic rigidity of 5.528 Tm, optimal for nuclei with $A/Z \approx 1.965$. Every 25 s, a cocktail beam including the nuclides of interest was injected into the CSRe. About 36 ions were stored in each injection.

Two identical time-of-flight (TOF) detectors were installed 18 m apart in a straight section of the CSRe [29]. Each detector consists of a thin carbon foil ($\phi 40$ mm, $18 \mu\text{g}/\text{cm}^2$) and a set of microchannel plates (MCPs). By penetrating the carbon foil, the ions yielded secondary electrons which were guided to the MCPs. Fast timing signals from both MCPs were recorded by an oscilloscope with a sampling rate of 50 GHz. The measurement time was 400 μs after an injection trigger, corresponding to ~ 600 revolutions of the ions. From the recorded timing signals, the revolution time and velocity of every ion were determined simultaneously using the procedure described in [30,31]. Signal processing and particle identification were done following the procedures in [32].

Given the revolution time T and velocity v , the magnetic rigidity $B\rho$ and orbit length C of the stored ions are determined according to

$$B\rho = \frac{m}{q}\gamma v, \quad \text{and} \quad C = Tv, \quad (1)$$

where the Lorentz factor $\gamma = 1/\sqrt{1 - \beta^2}$ with β being the particle velocity in the unit of the speed of light in vacuum. $B\rho$ and C are correlated quantities, which characterize the motion of all stored ions in the ring.

The nuclei with well-known masses, i.e., with mass uncertainties of $\sigma < 5$ keV [33], were used to construct the $B\rho(C)$ function through a least-square fit to all experimental $\{B\rho_{\text{exp}}, C_{\text{exp}}\}$ data obtained for each such ion. Then, the m/q value of any ion (i) including the unknown-mass nuclei was derived directly according to

$$\left(\frac{m}{q}\right)_{\text{exp}}^i = \frac{B\rho(C_{\text{exp}}^i)}{(\gamma v)_{\text{exp}}^i}, \quad i = 1, 2, 3, \dots \quad (2)$$

Equation (2) is the basic formula of the $B\rho$ -IMS technique [34,35], and the $B\rho(C)$ function is a universal mass calibration curve valid for all stored ions.

All individual m/q values were put into a histogram forming an integrated m/q spectrum. Part of the spectrum is presented in Fig. 1(a). Peaks of nuclei with nearly identical m/q ratios may overlap. To obtain the m/q values from overlapped peaks, we introduced a Z -dependent parameter defined as

$$U = \epsilon \bar{H} = \frac{N_{\text{exp}} \sum H_i}{N_{\text{total}} N_{\text{exp}}}, \quad (3)$$

which was extracted from the timing signals of the TOF detectors. Here, ϵ is the detection efficiency for a specific ion, $\bar{H}(H_i)$ the average (individual) signal amplitude of that ion, N_{exp} the number of timing signals created by the passing ion, and N_{total} the total revolution number. The parameter U has been used to decompose overlapping peaks [36,37], and the two series of $N = Z - 2$ and $N = Z - 1$ nuclei are clearly separated, see Fig. 1(b).

Most of the nuclides observed have well-known masses, and those with $Z \geq 15$ were used for calibration, i.e., to construct the $B\rho(C)$ function. Furthermore, each of the calibrants was supposed to be unknown, and its mass was redetermined by using the remaining reference nuclides as calibrants. The redetermined mass excesses (MEs) were utilized to calculate the normalized chi-square χ_n . The resultant $\chi_n = 1.066$ is within the expected interval of 1 ± 0.139 , indicating that no additional systematic errors are needed at 1σ confidence level.

The present work yields new masses for six $N = Z - 2$ nuclides, among which the masses of ^{62}Ge , ^{64}As , ^{66}Se , and ^{70}Kr are obtained for the first time. The new masses, see Table I, are systematically smaller than the values extrapolated in AME'20 [33,38]. Masses of six $N = Z - 1$ nuclides ^{61}Ga , ^{63}Ge , ^{65}As , ^{67}Se , ^{71}Kr , and ^{75}Sr are redetermined with higher precision. Overall, the redetermined masses are in agreement (within about 2 standard deviations) with literature values [33,38]. The masses of $^{60,61}\text{Ga}$

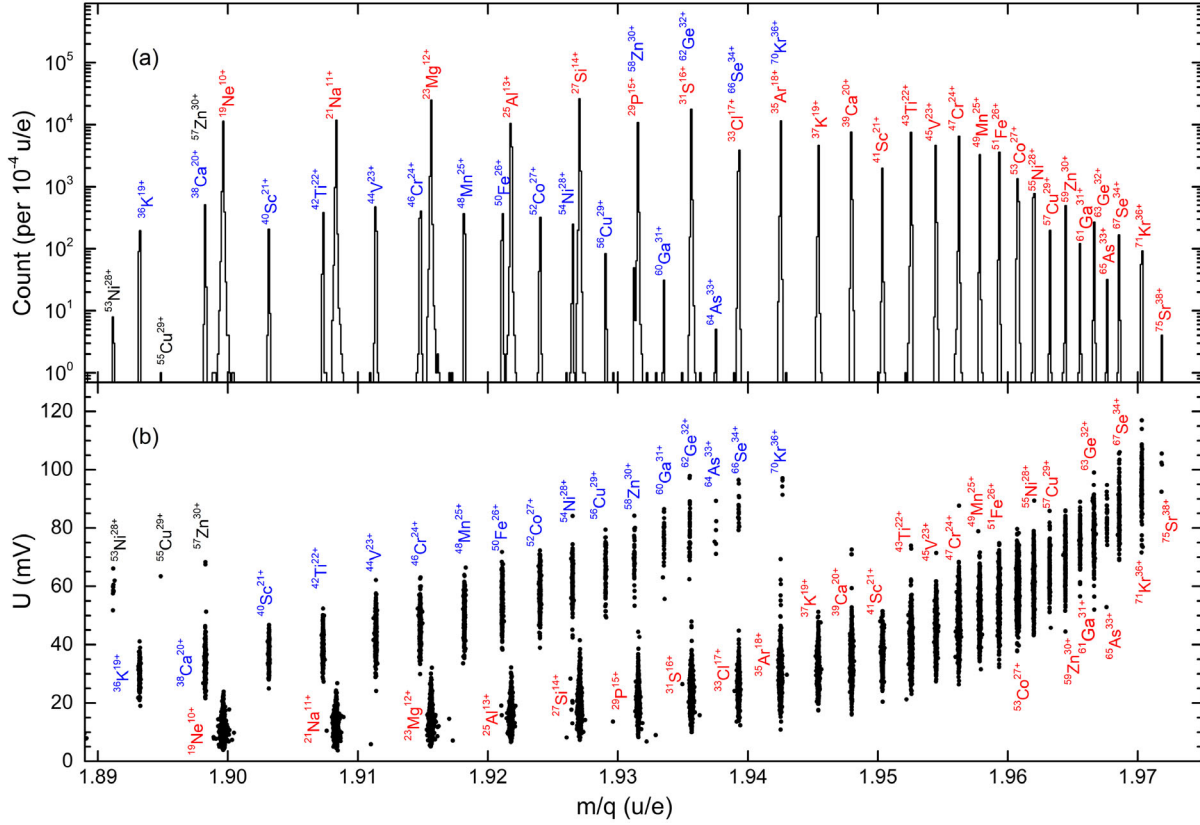


FIG. 1. Part of the m/q spectrum (a) and the corresponding scatter plot of U versus m/q (b). The spectrum is enlarged in the region of $m/q = 1.889\text{--}1.975$ u/e. The ion species are also indicated. Note that the unresolved $^{57}\text{Zn}^{30+}$, $^{62}\text{Ge}^{32+}$, $^{66}\text{Se}^{34+}$, and $^{70}\text{Kr}^{36+}$ in the m/q spectrum are completely separated from $^{38}\text{Ca}^{20+}$, $^{31}\text{S}^{16+}$, $^{37}\text{Cl}^{17+}$, and $^{35}\text{Ar}^{18+}$, respectively, in the plot of U versus m/q .

were measured recently by the TITAN MR-TOF mass spectrometer [39]. Our mass of ^{60}Ga is in excellent agreement with the reported $\text{ME}(^{60}\text{Ga}) = -40\,005(30)$ keV, and the mass of ^{61}Ga deviates by $-54(24)$ keV [39].

TABLE I. Mass excess (ME) values obtained in this work (IMS). Also listed are the number of counts, the ME values in AME'20 [33,38], and the mass differences $\Delta\text{ME} = \text{ME}_{\text{IMS}} - \text{ME}_{\text{AME}'20}$.

Atom	Counts	ME_{IMS} (keV)	$\text{ME}_{\text{AME}'20}$ (keV)	ΔME (keV)
^{58}Zn	51	-42 248(36)	-42 300(50)	51(62)
^{60}Ga	32	-40 034(46)	-39 590(200) ^b	-440(210) ^b
^{62}Ge	47	-42 289(37)	-42 140(140) ^b	-150(140) ^b
$^{64}\text{As}^{\text{a}}$	6	-39 710(110)	-39 530(200) ^b	-170(230) ^b
$^{66}\text{Se}^{\text{a}}$	20	-41 982(61)	-41 660(200) ^b	-320(210) ^b
^{70}Kr	4	-41 320(140)	-41 100(200) ^b	-220(250) ^b
^{61}Ga	124	-47 168(21)	-47 135(38)	-33(43)
$^{63}\text{Ga}^{\text{a}}$	279	-46 978(15)	-46 921(37)	-57(40)
$^{65}\text{As}^{\text{a}}$	33	-46 806(42)	-46 937(85)	131(95)
$^{67}\text{Se}^{\text{a}}$	174	-46 549(20)	-46 580(67)	32(70)
^{71}Kr	148	-46 056(24)	-46 327(129)	270(130)
^{75}Sr	4	-46 200(150)	-46 620(220)	420(260)

^aUsed for constraining the ^{64}Ge rp-process waiting point [40].

^bExtrapolated values from [33,38].

We note that the masses of ^{63}Ge , $^{64,65}\text{As}$, and $^{66,67}\text{Se}$ are as well utilized elsewhere to constrain the rapid proton capture process (rp-process) at ^{64}Ge , see Ref. [40].

The newly measured masses give δV_{pn}^{ee} values via [5]

$$\delta V_{pn}^{ee}(Z, N) = \frac{1}{4} [B(Z, N) - B(Z, N - 2) - B(Z - 2, N) + B(Z - 2, N - 2)], \quad (4)$$

for the nuclei with $N = Z = \text{even}$ (δV_{pn}^{ee}), and

$$\delta V_{pn}^{oo}(Z, N) = [B(Z, N) - B(Z, N - 1) - B(Z - 1, N) + B(Z - 1, N - 1)], \quad (5)$$

for those with $N = Z = \text{odd}$ (δV_{pn}^{oo}). The results are shown in Fig. 2 together with the δV_{pn} values extracted using currently available mass models [41–49].

Our results show that the increasing trend of δV_{pn}^{oo} beyond $Z = 28$ (red dashed line) is definitely established, which was suggested as an indication of the restoration of the pseudo-SU(4) symmetry in the fp shell [17,18], while δV_{pn}^{ee} follows the decreasing trend (red solid line) as reported in the lower mass region [4,13]. The latter is

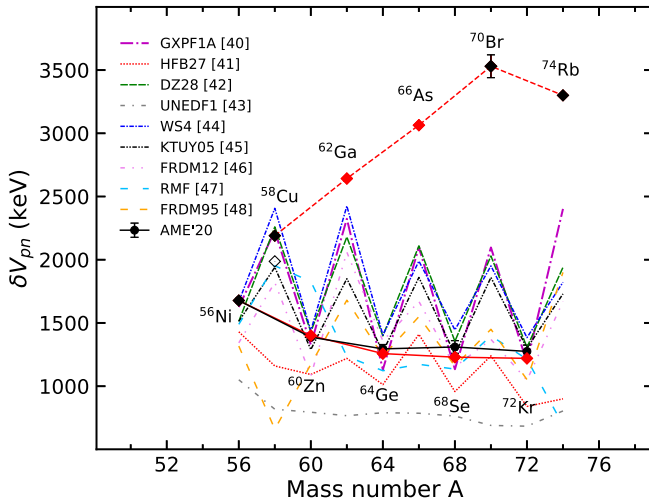


FIG. 2. Experimental δV_{pn} for $N = Z$ nuclei beyond $A = 56$ and comparison to different mass model predictions [41–49]. Red lines are to guide the eye. Red symbols indicate that one of the masses given in Table I was used. δV_{pn} of ^{58}Cu using the binding energy of the $T = 1, J^\pi = 0^+$ excited state [33] is marked with open diamond. $\text{ME}(^{70}\text{Br}) = -52\,030(80)$ keV is taken from [50,51]. δV_{pn} values obtained by using the extrapolated masses in AME'20 [33,38] are connected by the black solid line.

in contrary to the expectation of pseudo-SU(4) symmetry [5,16]. The increasing trend of δV_{pn} can be caused by enhanced overlaps of proton and neutron wave functions [13,14,52] or the growing nuclear deformation [9,53]. However, all these mechanisms ought to induce harmonized falling or rising of both δV_{pn}^{oo} and δV_{pn}^{ee} with changing A in the same region. Obviously, it is not the case as shown in Fig. 2.

We have extracted the δV_{pn} values using the predicted masses of frequently used mass models [41–49], and found that none of the models can reproduce the bifurcation of δV_{pn} , see Fig. 2. Understanding this intriguing phenomenon remains a theoretical challenge.

As protons and neutrons in $N = Z$ nuclei occupy identical orbits j , they can couple to isospin $T = 1$ with angular momentum $J = 0, 2, \dots, 2j - 1$, or to $T = 0$ with $J = 1, 3, \dots, 2j$ [54]. The ground states of odd-odd nuclei ^{62}Ga , ^{66}As , ^{70}Br , and ^{74}Rb were identified to be $(T, J^\pi) = (1, 0^+)$ [33,38]. This implies that the last proton and neutron couple to a $T = 1$ pn pair with $J = 0$. Therefore, the δV_{pn}^{oo} value deduced from Eq. (5) is in fact the $T = 1$ pn pairing energy, which is expected to be equal to the pp - and nn -pairing energies due to the charge independence of nuclear forces. Among all the coupled $T = 1$ states with $J = 0, 2, \dots, 2j - 1$, the pn interaction of the $J = 0$ state (pn pairing) is the most attractive (see Fig. 2 in [54]), and hence this component gives rise to the ground states of the odd-odd nuclei.

In the even-even $N = Z$ nuclei, the deduced δV_{pn}^{ee} values from Eq. (4) consist of weighted contributions from both

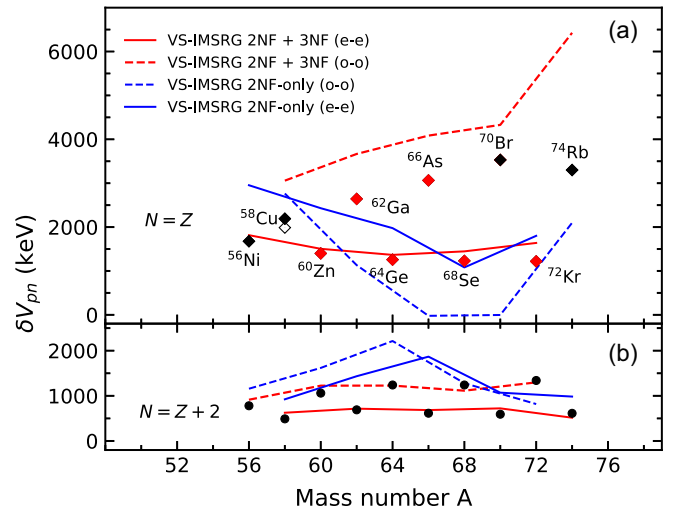


FIG. 3. Experimental δV_{pn} for (a) $N = Z$ and (b) $N = Z + 2$ nuclei beyond $A = 56$ and comparison with the *ab initio* calculations. Data uncertainties are within the size of the symbols. δV_{pn} values from *ab initio* calculations using 2NF + 3NF and 2NF only are plotted as red and blue lines (solid lines for even-even and dashed lines for odd-odd), respectively.

$T = 1$ and $T = 0$ channels of the pn interactions involving all possible J [55]. Indeed, by including both $T = 0$ and $T = 1$ components of the pn interaction, the magnitude and the decreasing trend in δV_{pn}^{ee} for the sd -shell nuclei have been well reproduced by shell model calculations using the universal sd -shell (USD) interaction [4]. The relatively smaller δV_{pn}^{ee} compared to δV_{pn}^{oo} can thus be attributed to the weighted $J \neq 0$ components of the pn interaction.

To understand the bifurcation of δV_{pn} , we have performed an *ab initio* valence-space in-medium similarity renormalization group (VS-IMSRG) calculation using a chiral interaction with two-nucleon force (2NF) at $N^3\text{LO}$ and three-nucleon force (3NF) at $N^2\text{LO}$, named EM1.8/2.0 [56], which can globally reproduce the ground-state energies [21,57]. Using the VS-IMSRG, the fp -shell effective Hamiltonian was decoupled assuming ^{40}Ca to be the core. The final diagonalization of the valence-space Hamiltonian was carried out using KSHELL [58]. The theoretical δV_{pn} in Fig. 3 are obtained from Eqs. (4) or (5) using the calculated binding energies.

As shown in Fig. 3(b), our calculations with 3NF included excellently reproduce the experimental δV_{pn} for the $N = Z + 2$ nuclei, showing the capability of the *ab initio* approach. For the $N = Z$ nuclei, the calculations well reproduce the δV_{pn}^{ee} data from ^{56}Ni to ^{72}Kr , which decrease slightly with increasing A . As both $T = 0$ and $T = 1$ pn correlations are included naturally in the *ab initio* calculation, reasonable agreement with experimental δV_{pn}^{oo} values is also obtained from ^{58}Cu to ^{70}Br , and in particular, the increasing trend of δV_{pn}^{oo} with changing A is well reproduced. We emphasize that our calculations give an isospin of $T = 1$ to the ground states of odd-odd nuclei, consistent with experimental assignment except for ^{58}Cu .

To understand the role played by 3NF, calculations have been performed using only a chiral 2NF at N³LO. The calculations using 2NF-only show different results with respect to those with 3NF included in three aspects at least. First, the agreements with experimental δV_{pn} are worse than those using 2NF + 3NF, see the blue lines in Fig. 3. Second, the isospins of ground states in odd-odd ⁶²Ga through ⁷⁴Rb are all predicted to be $T = 0$, which conflicts with experimental assignments. Third, opposite to the result with 3NF included, the δV_{pn}^{oo} value is smaller than δV_{pn}^{ee} for $N = Z$ nuclei, and both of them decrease or increase synchronously with A , see blue lines in Fig. 3. The results are again in conflict with experiment.

Inspecting the results of *ab initio* calculations with and without 3NF included, it is obvious that 3NF has a significant impact on the behavior of δV_{pn} . The 3NF enhances the pn correlations in $N = Z$ nuclei with a stronger $T = 1$ enhancement. In the ground states of odd-odd $N = Z$ nuclei, only $T = 1$ pairing appears, and hence the effect of 3NF on δV_{pn}^{oo} is more significant, resulting in the isospin inversion of the ground states and the increased trend of δV_{pn}^{oo} . In the even-even $N = Z$ nuclei, both $T = 1$ and $T = 0$ components of pn correlation contribute to δV_{pn}^{ee} , and the calculation with 3NF gives much better description of the δV_{pn}^{ee} than the calculation without 3NF.

Finally, it is worth noting that from the calculations with 3NF included, theoretical δV_{pn}^{oo} values of $N = Z$ nuclei are systematically larger than those extracted from experimental masses, e.g., for ⁷⁴Rb (see Fig. 3). Such a general overestimation in δV_{pn}^{oo} can also be observed in the lighter mass region if one uses the theoretical binding energies in [21]. The overestimation becomes significant when approaching the shell closure. The underlying reason has not been understood yet and thus calls for further experimental and theoretical studies.

In conclusion, the masses of 12 upper fp -shell $N = Z - 2$ and $N = Z - 1$ nuclei were measured with high accuracy using the newly developed $B\rho$ -IMS [34]. The δV_{pn} systematics was completed up to $Z = 37$, $N = Z$ nuclei. Beyond $Z = 28$, δV_{pn}^{oo} (δV_{pn}^{ee}) distinctly increases (decreases) with increasing A . This bifurcation was observed for the first time, which could not be reproduced by available mass models and also opposes the expectation of the restoration of pseudo-SU(4) symmetry in the upper fp shell. To understand the observed phenomenon, we have performed *ab initio* calculations using the chiral nuclear force with and without three-nucleon interaction included. The calculations show that the three-nucleon force enhances the strength of pn pairing correlations compared to the results with only two-nucleon interaction. The enhancement of $T = 1$ pn pairing is stronger than that of $T = 0$ pn pairing, reproducing the bifurcation in δV_{pn} . However, the calculated δV_{pn} for odd-odd $N = Z$

nuclei are systematically overestimated. This implies that state-of-the-art *ab initio* approaches need further improvement, and accurate masses of nuclei along $N = Z$ provide an important testing ground.

We thank the staff of the accelerator division of IMP for providing the stable ⁷⁸Kr beam. This work is supported in part by the National Key R&D Program of China (Grant No. 2018YFA0404401), the Strategic Priority Research Program of Chinese Academy of Sciences (Grant No. XDB34000000), the CAS Project for Young Scientists in Basic Research (Grant No. YSBR-002), National Key R&D Program of China (Grant No. 2021YFA1601500), and the NSFC (Grants No. 12135017, No. 12121005, No. 11961141004, No. 11905259, No. 11905261, No. 11605248, No. 11975280, No. 11835001, No. 11921006, No. 12035001). Y. M. X. and C. Y. F. acknowledge support from CAS ‘‘Light of West China’’ Program. R. J. C. is supported by the International Postdoctoral Exchange Fellowship Program 2017 by the Office of China Postdoctoral Council (No. 60 Document of OCPC, 2017). Y. A. L. is supported by the European Research Council (ERC) under the EU Horizon 2020 research and innovation programme (ERC-CG 682841 ‘‘ASTRUM’’).

*yhzhang@impcas.ac.cn

†zxh@impcas.ac.cn

‡frxu@pku.edu.cn

- [1] K. Blaum, *Phys. Rep.* **425**, 1 (2006).
- [2] T. Yamaguchi, H. Koura, Y. Litvinov, and M. Wang, *Prog. Part. Nucl. Phys.* **120**, 103882 (2021).
- [3] J.-Y. Zhang, R. Casten, and D. Brenner, *Phys. Lett. B* **227**, 1 (1989).
- [4] D. Brenner, C. Wesselborg, R. Casten, D. Warner, and J.-Y. Zhang, *Phys. Lett. B* **243**, 1 (1990).
- [5] P. Van Isacker, D. D. Warner, and D. S. Brenner, *Phys. Rev. Lett.* **74**, 4607 (1995).
- [6] I. Talmi, *Rev. Mod. Phys.* **34**, 704 (1962).
- [7] P. Federman and S. Pittel, *Phys. Lett.* **69B**, 385 (1977).
- [8] R. F. Casten, *Phys. Rev. Lett.* **54**, 1991 (1985).
- [9] R. B. Cakirli and R. F. Casten, *Phys. Rev. Lett.* **96**, 132501 (2006).
- [10] K. Heyde, P. Van Isacker, R. Casten, and J. Wood, *Phys. Lett.* **155B**, 303 (1985).
- [11] P. Federman and S. Pittel, *Phys. Lett.* **77B**, 29 (1978).
- [12] R. B. Cakirli, D. S. Brenner, R. F. Casten, and E. A. Millman, *Phys. Rev. Lett.* **94**, 092501 (2005).
- [13] D. S. Brenner, R. B. Cakirli, and R. F. Casten, *Phys. Rev. C* **73**, 034315 (2006).
- [14] L. Chen *et al.*, *Phys. Rev. Lett.* **102**, 122503 (2009).
- [15] Y. H. Zhang *et al.*, *Phys. Rev. C* **98**, 014319 (2018).
- [16] P. Van Isacker, O. Juillet, and F. Nowacki, *Phys. Rev. Lett.* **82**, 2060 (1999).
- [17] P. Schury *et al.*, *Phys. Rev. C* **75**, 055801 (2007).
- [18] I. Mardor *et al.*, *Phys. Rev. C* **103**, 034319 (2021).

- [19] D. Warner, M. Bentley, and P. V. Isacker, *Nat. Phys.* **2**, 311 (2006).
- [20] A. T. Gallant *et al.*, *Phys. Rev. Lett.* **109**, 032506 (2012).
- [21] S. R. Stroberg, J. D. Holt, A. Schwenk, and J. Simonis, *Phys. Rev. Lett.* **126**, 022501 (2021).
- [22] J. D. Holt, J. Menéndez, and A. Schwenk, *Phys. Rev. Lett.* **110**, 022502 (2013).
- [23] M. Mougeot *et al.*, *Nat. Phys.* **17**, 1099 (2021).
- [24] J. Xia *et al.*, *Nucl. Instrum. Methods Phys. Res., Sect. A* **488**, 11 (2002).
- [25] W. Zhan, H. Xu, G. Xiao, J. Xia, H. Zhao, and Y. Yuan, *Nucl. Phys.* **A834**, 694c (2010).
- [26] M. Hausmann *et al.*, *Nucl. Instrum. Methods Phys. Res., Sect. A* **446**, 569 (2000).
- [27] Y. H. Zhang, Y. A. Litvinov, T. Uesaka, and H. S. Xu, *Phys. Scr.* **91**, 073002 (2016).
- [28] M. Steck and Y. A. Litvinov, *Prog. Part. Nucl. Phys.* **115**, 103811 (2020).
- [29] X.-L. Yan, R.-J. Chen, M. Wang, Y.-J. Yuan, J.-D. Yuan, S.-M. Wang, G.-Z. Cai, M. Zhang, Z.-W. Lu, C.-Y. Fu *et al.*, *Nucl. Instrum. Methods Phys. Res., Sect. A* **931**, 52 (2019).
- [30] X. Tu *et al.*, *Nucl. Instrum. Methods Phys. Res., Sect. A* **654**, 213 (2011).
- [31] X. Zhou, M. Zhang, M. Wang, Y. H. Zhang, Y. J. Yuan, X. L. Yan, X. H. Zhou, H. S. Xu, X. C. Chen, Y. M. Xing *et al.*, *Phys. Rev. Accel. Beams* **24**, 042802 (2021).
- [32] Y. Xing, Y. Zhang, M. Wang, Y. Litvinov, R. Chen, X. Chen, C. Fu, H. Li, P. Shuai, M. Si *et al.*, *Nucl. Instrum. Methods Phys. Res., Sect. A* **941**, 162331 (2019).
- [33] M. Wang, W. Huang, F. Kondev, G. Audi, and S. Naimi, *Chin. Phys. C* **45**, 030003 (2021).
- [34] M. Wang *et al.*, *Phys. Rev. C* **106**, L051301 (2022).
- [35] M. Zhang *et al.*, *Eur. Phys. J. A* **59**, 27 (2023).
- [36] P. Shuai *et al.*, *Phys. Lett. B* **735**, 327 (2014).
- [37] X. Zhou, M. Wang, Y.-H. Zhang, H.-S. Xu, Y.-J. Yuan, J.-C. Yang, Y. A. Litvinov, S. A. Litvinov, B. Mei, X.-L. Yan *et al.*, *Nucl. Sci. Tech.* **32**, 37 (2021).
- [38] F. Kondev, M. Wang, W. Huang, S. Naimi, and G. Audi, *Chin. Phys. C* **45**, 030001 (2021).
- [39] S. F. Paul, J. Bergmann, J. D. Cardona, K. A. Dietrich, E. Dunling, Z. Hockenbery, C. Hornung, C. Izzo, A. Jacobs, A. Javaji *et al.*, *Phys. Rev. C* **104**, 065803 (2021).
- [40] X. Zhou *et al.* *Nat. Phys.* (2023), 10.1038/s41567-023-02034-2.
- [41] M. Honma, T. Otsuka, B. A. Brown, and T. Mizusaki, *Eur. Phys. J. A* **25**, 499 (2005).
- [42] S. Goriely, N. Chamel, and J. M. Pearson, *Phys. Rev. C* **88**, 061302(R) (2013).
- [43] J. Duflo and A. P. Zuker, *Phys. Rev. C* **52**, R23 (1995).
- [44] M. Kortelainen, J. McDonnell, W. Nazarewicz, P.-G. Reinhard, J. Sarich, N. Schunck, M. V. Stoitsov, and S. M. Wild, *Phys. Rev. C* **85**, 024304 (2012).
- [45] N. Wang, M. Liu, X. Wu, and J. Meng, *Phys. Lett. B* **734**, 215 (2014).
- [46] T. Kawano, S. Chiba, and H. Koura, *J. Nucl. Sci. Technol.* **43**, 1 (2006).
- [47] P. Möller, A. Sierk, T. Ichikawa, and H. Sagawa, *At. Data Nucl. Data Tables* **109–110**, 1 (2016).
- [48] L. Geng, H. Toki, and J. Meng, *Prog. Theor. Phys.* **113**, 785 (2005).
- [49] P. Moller, J. Nix, W. Myers, and W. Swiatecki, *At. Data Nucl. Data Tables* **59**, 185 (1995).
- [50] M. Karny, L. Batist, D. Jenkins, M. Kavatsyuk, O. Kavatsyuk, R. Kirchner, A. Korgul, E. Roeckl, and J. Żylicz, *Phys. Rev. C* **70**, 014310 (2004).
- [51] D. G. Jenkins *et al.*, *Phys. Rev. C* **65**, 064307 (2002).
- [52] R. B. Cakirli, K. Blaum, and R. F. Casten, *Phys. Rev. C* **82**, 061304(R) (2010).
- [53] D. Bonatsos, S. Karampagia, R. B. Cakirli, R. F. Casten, K. Blaum, and L. A. Susam, *Phys. Rev. C* **88**, 054309 (2013).
- [54] S. Frauendorf and A. Macchiavelli, *Prog. Part. Nucl. Phys.* **78**, 24 (2014).
- [55] N. Zeldes, *Phys. Lett. B* **429**, 20 (1998).
- [56] K. Hebeler, S. K. Bogner, R. J. Furnstahl, A. Nogga, and A. Schwenk, *Phys. Rev. C* **83**, 031301(R) (2011).
- [57] T. Miyagi, S. R. Stroberg, P. Navrátil, K. Hebeler, and J. D. Holt, *Phys. Rev. C* **105**, 014302 (2022).
- [58] N. Shimizu, T. Mizusaki, Y. Utsuno, and Y. Tsunoda, *Comput. Phys. Commun.* **244**, 372 (2019).